Mitochondrial energetic metabolism: A simplified model of TCA cycle with ATP production

Christine Nazaret [a,*] , Margit Heiske [c], Kevin Thurley [c], Jean-Pierre Mazat [b]

[a] IMB UMR CNRS 5251-ESTBB, Université de Bordeaux 2, 146 rue Léo-Saignat, F 33076 Bordeaux-cedex, France
[b] Inserm U688, Université de Bordeaux 2, 146 rue Léo-Saignat, F 33076 Bordeaux-cedex, France
[c] Humboldt Universität, Berlin, Germany

A B S T R A C T

Mitochondria play a central role in cellular energetic metabolism. The essential parts of this metabolism are the tricarboxylic acid (TCA) cycle, the respiratory chain and the adenosine triphosphate (ATP) synthesis machinery. Here a simplified model of these three metabolic components with a limited set of differential equations is presented. The existence of a steady state is demonstrated and results of numerical simulations are presented. The relevance of a simple model to represent actual in vivo behavior is discussed.

© 2008 Elsevier Ltd. All rights reserved.

1. Introduction

Mitochondria are small organelles found in most living cells. They are sometimes described as cellular power plants because one of their functions is to convert organic materials into energy in the form of adenosine triphosphate (ATP). A mitochondrion is composed of an inner space called matrix containing a highly concentrated mixture of enzymes and chemical species. The matrix is enclosed by two membranes with very different properties. The inner membrane is highly impermeable to ions and molecules which require special membrane transporters to enter and exit the matrix, whereas the outer membrane is permeable to many molecules. In this work, only the matrix and the inner mitochondrial membrane will be considered. The mitochondrial energy metabolism involves three main sets of biochemical reactions: the tricarboxylic acid cycle (TCA cycle or Krebs cycle), the respiratory chain (RC) and the ATP synthesis machinery (see Fig. 1). The mitochondrial energetic metabolism has extensively been modeled since the pioneering works of Garfinkel (1971a, b), Wilson et al. (1977) and Bohnensack (1981).

Korzeniewski (1991) developed a more complex model also based on ordinary differential equations, which was applied to isolated mitochondria or to intact tissues (muscle, heart and liver). Cortassa et al. (2003) developed a model including the TCA cycle, the transports of Ca^{2+} across the mitochondrial inner membrane and the regulation of dehydrogenases by Ca^{2+}. The interest of this model is to match the supply of mitochondrial energy to the cellular demand, through the variations of intracellular and intramitochondrial Ca^{2+}. More recently, Beard (2005) and Wu et al. (2007) proposed "A biophysical model of the mitochondrial respiratory system and oxidative phosphorylation" mainly applied to cardiac mitochondria.

But as the set of equations of the models is usually very large, mathematical analysis of such models is quite hard and rarely performed. Our aim is to develop a simple model of the mitochondrial energetic metabolism based on a limited set of differential equations. It involves a simple phenomenological representation of the RC and of ATP synthesis machinery by only one phenomenological equation in each case and a reduced model of TCA cycle by lumping consecutive reactions while keeping the possible design of this part of the metabolism in two sub-cycles.

With this very simple and reduced model, our goal is to simulate the most important properties of the three-part mitochondrial energy metabolism, i.e. (i) the links among the

* Corresponding author. Tel.: +33 5 57 57 11 10; fax: +33 5 57 57 46 43.
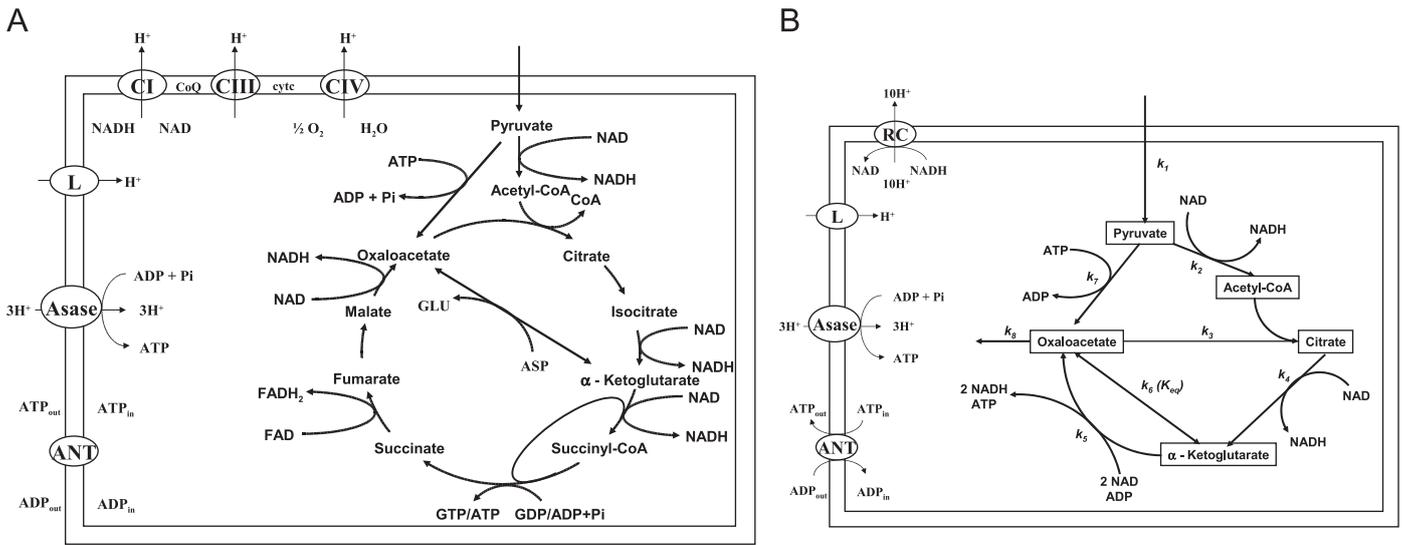 *E-mail address:* nazaret@sm.u-bordeaux2.fr (C. Nazaret).

Fig. 1. Essential parts of mitochondrial energetic metabolism (A) and our model (B).

three parts: ATP synthesis, RC and TCA cycle and (ii) the coordinate response when ATP demand is varied: responses of the transmembrane potential, of the rate of respiration and of the flux through the TCA cycle. In addition, we will impose (iii) keeping in a physiological range the concentrations of the few intermediate metabolites considered in TCA cycle. We will give mathematical properties of the model (existence of a unique non-negative solution globally defined on $[0, +\infty)$, existence of stationary state). Then, we will perform some simulations to illustrate the interest of using a simple model to emphasize actual in vivo behaviors.

2. The model

The essential parts of the mitochondrial energetic metabolism responsible for ATP production are summarized in Fig. 1A. They involve the TCA cycle, the RC which generates a proton gradient, the ATP synthase (Asase), the adenine-nucleotide-translocator (ANT) and a proton leak through the membrane (L). We will describe in the following how we model these different parts in a simplified way.

2.1. Inside the matrix: TCA cycle modeling

The TCA cycle is a central part of the energetic metabolism that contributes to the generation of ATP by the chemical breakdown of carbohydrates, fats and proteins. It is a series of chemical reactions catalyzed by enzymes occurring in the inside of mitochondria, called the matrix, and which can be disposed circularly (see Fig. 1A). It has been recognized since a long time that the TCA cycle can be split into two mini-cycles by transaminases linking directly α-ketoglutarate to oxaloacetate (Rustin et al., 1997; Kondracheva and Doliba, 1989; Parlo and Coleman, 1984). In our model the two mini-cycles are assembled each in only one reaction (see Fig. 1B): one reaction representing aconitase plus isocitrate dehydrogenase (reaction (4) where reaction i corresponds to reaction $\xrightarrow{k_i}$ of Fig. 1B), the other assembling α-ketoglutarate dehydrogenase, succinyl-CoA synthase, fumarase and malate dehydrogenase (reaction (5)). Both reactions are thought to be irreversible because in each case, at least one of the elementary reactions is irreversible: reaction

(4) because isocitrate dehydrogenase is irreversible and also reaction (5) because succinate dehydrogenase, which is part of Complex II of the RC, is irreversible. One of the main features of the TCA cycle is the reduction of NAD to NADH. The reduction of one NAD can be attributed to the first assembling reaction (4) and two NAD are reduced by reaction (5). In addition another NAD reduction is linked to pyruvate dehydrogenase (reaction (2)) following the entry of pyruvate (reaction (1)) and is also irreversible (Berg et al., 2006). Another quasi-irreversible fate of pyruvate goes through the pyruvate carboxylase (reaction(7)); the quasi-irreversibility in this case is due to the very small concentration of oxaloacetate. The modeling of the rate equations by taking into account the "quasi-stationary state hypothesis" leads to quite sophisticated formulas (see Segel, 1975 for more details). For the sake of simplicity we use the mass action law as indicated below.

if irreversible $A + B \longrightarrow C + D$ $\dfrac{dC}{dt} = kAB$

otherwise reversible $A + B \longleftrightarrow C + D$ $\dfrac{dC}{dt} = k\left(AB - \dfrac{CD}{K_{eq}}\right)$

with k the rate of the forward reaction and K_{eq} the equilibrium constant of the reaction approximated by $K_{eq} = C_{eq}D_{eq}/A_{eq}B_{eq}$ where X_{eq} are the concentration of the species X at equilibrium (when the forward reaction rate equals the backward reaction rate).

In order that the system reaches a steady state, it is necessary to add some outputs to the TCA cycle through oxaloacetate (reaction (8)) and through NADH with a simple reaction representing the RC establishing a transmembrane potential $\Delta\psi$ modulated by a variable leak (L) and ATP synthesis (Asase). The effect of taking reactions (3) and (7) reversible has also been numerically studied.

2.2. At the membrane: the RC, the Asase, the ANT and the proton leak

- *Transmembrane potential.*
  The inner mitochondrial membrane is a selective barrier necessary for the coupling of the RC with the ATP synthesis. All of these mechanisms lead to changes in the proton concentration inside the mitochondrial matrix, which is generally lower than outside. This creates a difference of

potential $\Delta\psi$ through this membrane. We will consider this as a capacitor (as in Magnus and Keizer, 1997):
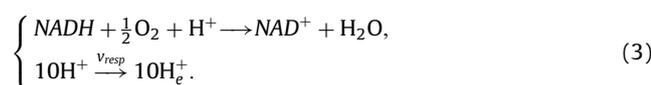
$$\Delta\psi = \frac{Q}{C}, \tag{1}$$

where Q is the charge and C the capacitance. Empirical values can be found in the literature for C (see Table 2) that directly converts the concentration of protons into an electrical potential $\Delta\psi = (H_e^+(t) - H^+(t))/C$ where the index e stands for outside of membrane. Thus, if we hypothesize that H_e^+ concentration is constant due to the large buffer volume outside the mitochondrial matrix, we obtain

$$\Delta\psi'(t) = -\frac{1}{C}H^{+'}(t). \tag{2}$$

- *Respiration.*
The RC is a very complex mechanism (see transmembrane complexes I–IV in Fig. 1) which is globally irreversible. We assemble all the RC complexes depicted in Fig. 1A in one entity (RC) in Fig. 1B with a rate function v_{resp}. The oxidation of one molecule of *NADH* provides the energy to transport ten protons outside the matrix into the intermembrane space. This can be simplified by two coupled reactions

$$\begin{cases} NADH + \frac{1}{2}O_2 + H^+ \longrightarrow NAD^+ + H_2O, \\ 10H^+ \xrightarrow{v_{resp}} 10H_e^+. \end{cases} \tag{3}$$

The rate of this reaction v_{resp} depends on the *NADH* concentration and on the protons H^+. Since the protons are charged, the dependence on H^+ is not only due to the difference of concentration in H^+ expressed as a ΔpH (osmotic effect) but also to an electrical effect expressed as a $\Delta\psi$ (see above). Both effects are summarized in the electrochemical potential difference in protons by the formula

$$\Delta\tilde{\mu} = \Delta\mu + F\Delta\psi, \tag{4}$$

where $\Delta\mu = 2.3RT(pH - pH_e) = 2.3RT\log(H_e^+/H^+)$ is the chemical part and $F\Delta\psi$ the electrical one with F the Faraday constant, R the gas constant and T the temperature in Kelvin. For liver mitochondria a $\Delta pH = pH_i - pH_e$ of 0.75 and a $\Delta\psi$ of 168 mV have been measured (Cortassa et al., 2003). At $T = 298$ K, we found $\Delta\mu \approx 4300$ J/mol and $F\Delta\psi \approx 16\,200$ J/mol which is approximately four times higher than $\Delta\mu$. Thus to simplify our modeling, the chemical effect $\Delta\mu$ is taken to be equal to 20% of $F\Delta\psi$, and thus the respiration rate will only depend on $\Delta\psi$ and of course, as mentioned above, on the *NADH* (or *NAD*) concentration. The rate function v_{resp} has two essential experimental properties: a Michaelis (hyperbolic) dependency of the *NADH* concentration with a saturating effect and a complete inhibition at high $\Delta\psi$ (the H^+ extrusion by the RC built the $\Delta\psi$ which acts against the extrusion of H^+). To calculate these dependencies (see for instance Magnus and Keizer, 1997; Bohnensack, 1981), we chose a differentiable function which describes these phenomenological properties of the respiration rate: a saturation curve for *NADH*, a nearly constant rate at $\Delta\psi$ of up to $\Delta\psi_m = 150$ mV, then a decrease towards 0 when $\Delta\psi$ increases (see Fig. 2)

$$v_{resp}(NAD, \Delta\psi) = k_{resp}\frac{N_t - NAD}{K + N_t - NAD}\frac{1}{1 + \exp(a(\Delta\psi - \Delta\psi_m))}, \tag{5}$$

where N_t is the total nicotinamide adenine dinucleotide concentration $N_t = NAD + NADH$ which is constant.
- *ATP synthesis.*
To produce *ATP* (the natural direction for the reaction is the hydrolysis of *ATP* to produce $ADP + Pi$ instead of the *ATP*
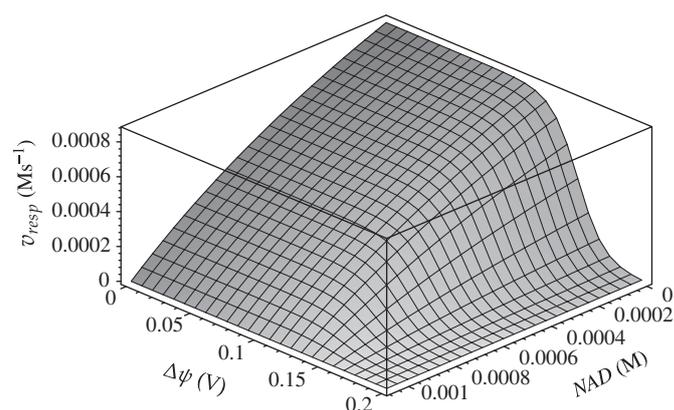

Fig. 2. Respiration rate modeling v_{resp}. $k_{resp} = 2.5$ mMs^{-1}, $K = 0.002$ M, $N_t = 1.07$ mM, $a = 100$ V^{-1}, $\Delta\psi_m = 0.15$ V.

synthesis), the Asase needs the energy supplied by the entry of three protons into the matrix space. This can be expressed by the two coupled reactions

$$\begin{cases} ADP + Pi \longleftrightarrow ATP + H_2O, \\ 3H_e^+ \xleftrightarrow{v_{ATP}} 3H^+. \end{cases} \tag{6}$$

An apparent equilibrium constant can be defined for the first reaction: $K_{app} = ATP_{eq}/(ADP_{eq}Pi_{eq})$(the convention is that H_2O is omitted in the equilibrium expression for K_{app} when reactions in dilute solutions are considered). We also define $\Gamma = ATP/(ADP\,Pi) = ATP/((A_t - ATP)Pi)$ where A_t is the total adenine nucleotide concentration $A_t = ATP + ADP$ which is constant. The free Gibbs energy variation of this reaction can be written as follows:

$$\Delta G_1 = -RT\ln\left(\frac{K_{app}}{\Gamma}\right). \tag{7}$$

The equilibrium constant is much more in favor of *ADP* ($K_{app} \approx 10^{-6}$). But mitochondria are able to maintain a ratio Γ which is far away from equilibrium to synthesize *ATP*: it requires an input of energy given by the second reaction $3H_e^+ \longleftrightarrow 3H^+$.
The overall free-energy change ΔG of the coupled reactions is equal to the sum of the free-energy changes of both: $\Delta G = \Delta G_1 + \Delta G_2$ where ΔG_2 is the free Gibbs energy of the second reaction, i.e. the energy released by the protons crossing the inner membrane. Because we hypothesized that the chemical potential variation of the proton is equal to 20% of $F\Delta\psi$, the free energy for one mole of protons to cross the inner membrane is given by

$$\Delta G_{transport} = 1.2F\Delta\psi. \tag{8}$$

Thus, the free Gibbs energy ΔG of the coupled reactions is given by (see Fig. 3)

$$\Delta G(ATP, \Delta\psi) = -RT\ln\left(\frac{K_{app}}{\Gamma}\right) - 3\Delta G_{transport}. \tag{9}$$

The direction of the reaction is given by the sign of ΔG. If $\Delta G < 0$, the phosphorylation of *ADP* in order to obtain *ATP* will proceed and the difference of potential $\Delta\psi$ will decrease. Otherwise the direction of the reaction will be in favor of *ATP* hydrolysis with proton extrusion and a building of the $\Delta\psi$ by the Asase. From $\Delta G = 0$, we evaluate a critical threshold for ATP depending on the potential $\Delta\psi$, denoted ATP_{crit} (see Fig. 4)

$$ATP_{crit}(\Delta\psi) = \frac{A_t}{1 + \dfrac{\exp\left(\dfrac{-3\Delta G_{transport}}{RT}\right)}{K_{app}Pi}} \tag{10}$$
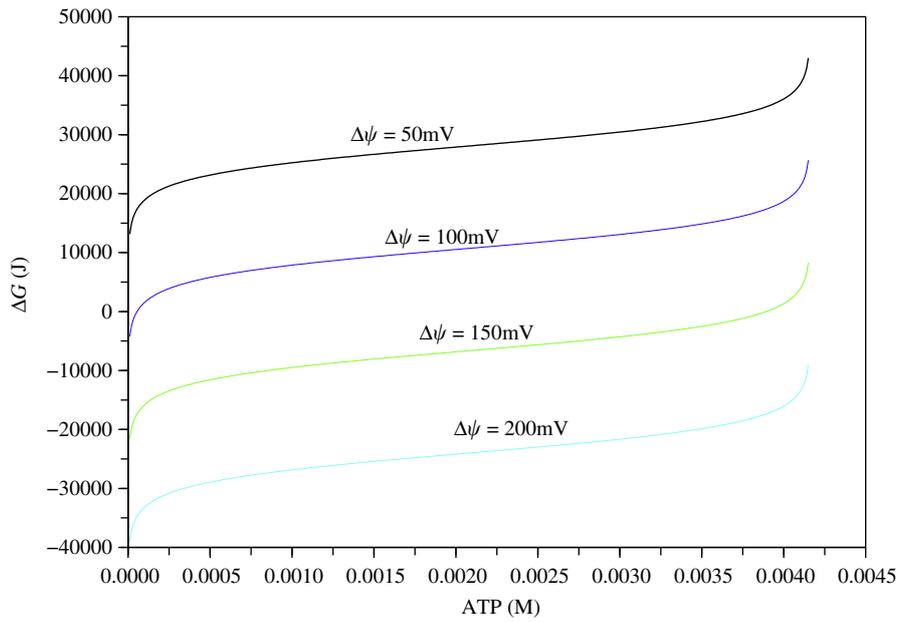
Fig. 3. Free Gibbs energy ΔG of ATP synthase as a function of *ATP* concentration at different $\Delta\psi$ values indicated on the curves. $R = 8.314\,\mathrm{J\,(mol\,K)^{-1}}$, $T = 298\,\mathrm{K}$, $F = 96\,485\,\mathrm{C\,mol^{-1}}$, $K_{app} = 4.4\,\mu\mathrm{M}$.
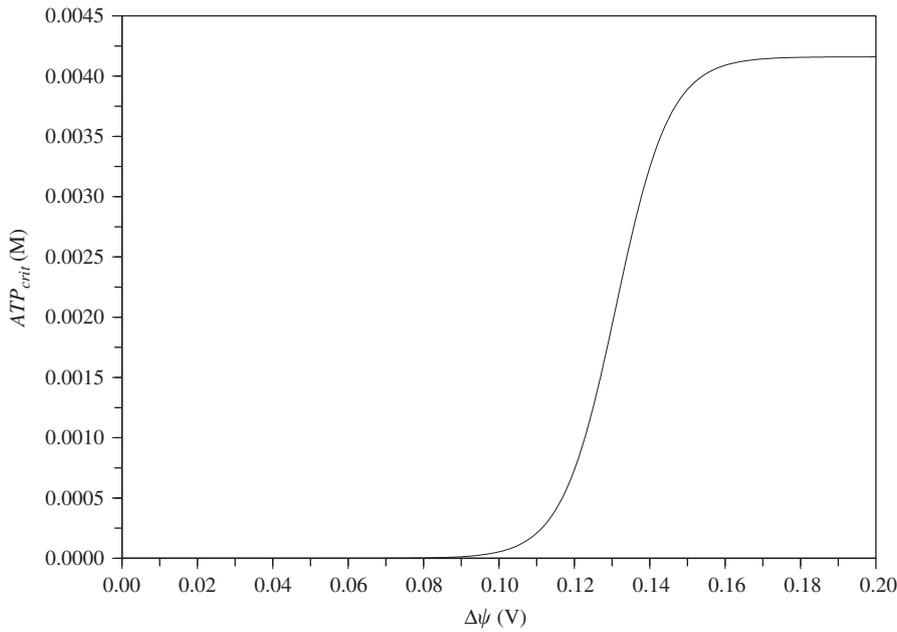

Fig. 4. Critical threshold ATP_{crit} as a function of $\Delta\psi$ values. ATP_{crit} is the value of *ATP* for which there is no synthesis or hydrolysis of *ATP* by ATP synthase. $A_t = 4.16\,\mathrm{mM}$, $R = 8.314\,\mathrm{J\,(mol\,K)^{-1}}$, $T = 298\,\mathrm{K}$, $K_{app} = 4.4\,\mu\mathrm{M}$, $Pi = 2.44\,\mathrm{mM}$.

and we set for the rate of reaction (see Fig. 5)

$$v_{ATP}(ATP, \Delta\psi) = k_{ATP}\left(\frac{2}{1 + \exp(b(ATP - ATP_{crit}(\Delta\psi)))} - 1\right). \quad (11)$$

If $ATP < ATP_{crit}$ then $v_{ATP} > 0$ and the phosphorylation of *ADP* will proceed. Otherwise the direction of the reaction will be in favor of *ATP* hydrolysis.

- The ANT is a mitochondrial protein that allows the exchange of *ATP* and *ADP* molecules across the inner mitochondrial membrane: $ATP + ADP_e \xrightarrow{v_{ANT}} ADP + ATP_e$. This mechanism can be simplified by

$$ATP \xrightarrow{v_{ANT}} ADP. \quad (12)$$

Since *ATP* and *ADP* exhibit a difference of charge (ATP^{4-} and ADP^{3-}), the exchange of *ADP* against *ATP* is accompanied by a concomitant decrease in $\Delta\psi$. For this reason, v_{ANT} also appears in the equation expressing the variation of $\Delta\psi$. We assume that the ANT process follows a simple law of mass action:

$$v_{ANT} = k_{ANT}ATP. \quad (13)$$

- The proton leak

$$H_e^+ \xrightarrow{v_{leak}} H^+. \quad (14)$$

Because the inner mitochondrial membrane cannot be entirely impermeable to protons we introduce a H$^+$ leak which is a function of $\Delta\psi$. We express this dependency by a simple linear

relationship:

$$v_{leak} = k_{leak} \Delta \psi. \tag{15}$$

2.3. The differential equations governing the system

The overall system is governed by the following set of eight differential equations:

$$Pyr'(t) = v_1 - v_2 - v_7, \tag{16}$$
$$AcCoA'(t) = v_2 - v_3, \tag{17}$$
$$Cit'(t) = v_3 - v_4, \tag{18}$$
$$KG'(t) = v_4 + v_6 - v_5, \tag{19}$$
$$OAA'(t) = v_5 + v_7 - v_3 - v_8 - v_6, \tag{20}$$
$$NAD'(t) = -v_2 - v_4 - 2v_5 + v_{resp,} \tag{21}$$
$$ATP'(t) = v_{ATP} - v_{ANT} + v_5 - v_7, \tag{22}$$
$$\Delta\psi'(t) = \frac{1}{C}(10v_{resp} - 3v_{ATP} - v_{leak} - v_{ANT}) \tag{23}$$

with the following rate equations

Fig. 5. Rate of ATP synthase v_{ATP}. $k_{atp} = 131.9\,\mathrm{mM\,s^{-1}}$, $b = 4\,\mathrm{M^{-1}}$.

$$v_1 = k_1, \quad v_2 = k_2 Pyr\,NAD, \quad v_3 = k_3 OAA\,AcCoA,$$
$$v_4 = k_4 Cit\,NAD, \quad v_5 = k_5 KG\,NAD(A_t - ATP), \quad v_6 = k_6(OAA - KG),$$
$$v_7 = k_7 Pyr\,ATP, \quad v_8 = k_8 OAA \quad v_{ANT} = k_{ANT}ATP,$$
$$v_{leak} = k_{leak}\Delta\psi,$$
$$v_{resp}(NAD, \Delta\psi) = k_{resp}\frac{N_t - NAD}{K + N_t - NAD}\frac{1}{1 + \exp(a(\Delta\psi - \Delta\psi_m))},$$
$$v_{ATP}(ATP, \Delta\psi) = k_{ATP}\left(\frac{2}{1 + \exp(b(ATP - ATP_{crit}(\Delta\psi)))} - 1\right),$$
$$ATP_{crit}(\Delta\psi) = \frac{A_t}{1 + \frac{\exp\left(\frac{-3\Delta G_{transport}}{RT}\right)}{K_{app}Pi}} \tag{24}$$

and a set of non-negative initial conditions

$$Pyr(0) > 0, \quad AcCoA(0) > 0, \dots, \Delta\psi(0) > 0, \tag{25}$$

where the parameters k_1–k_8, k_{resp}, k_{ATP}, k_{leak}, k_{ANT}, K_{eq}, K_{app}, C, K, $\Delta\psi_m$, a and b are constant and positive.

2.4. The steady state hypothesis and parameters of the model

In order to simulate actual experimental results, we used the Faraday constant $F = 96\,485\,\mathrm{C\,mol^{-1}}$, the gas constant $R = 8.314\,\mathrm{J/(mol\,K)}$, and the absolute temperature $T = 298\,\mathrm{K}$. During time intervals of several minutes and sometimes much more, it is experimentally observed that the concentrations of most of the metabolites are constant, which led us to look for stable stationary states mathematically and in the simulations. As regards the metabolite concentrations at steady state, we took the mean of several values found in the literature (between 10 and 20—see Table 1) which presumably corresponds to a physiological intermediate state between a resting state (state 4: no ATP synthesis) and an active state (state 3: maximal ATP synthesis). This state has sometimes been called state 3.5 (Korzeniewski et al., 2001).

Some other concentrations and equilibrium constants (which are taken to be constant in the model) were also found in the literature (see Table 2).
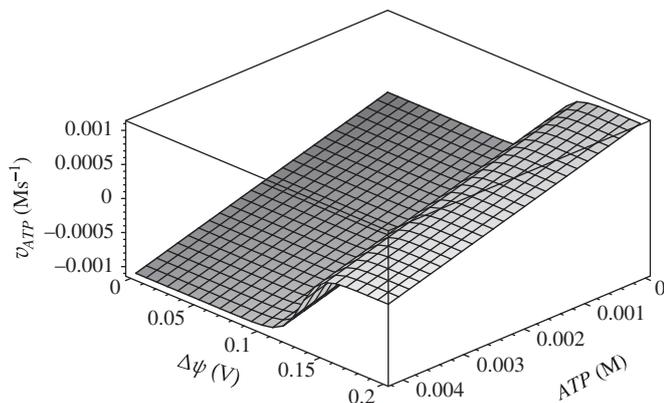
Table 1
Steady state concentration values at state 3.5.

Species or rates	Values in vivo	Unit[a]	References
$\overline{Pyr}$	0.140	mM	Bergmeyer (1974), Sies (1982), Garfinkel (1971a), Putman et al. (1999), Howarth et al. (2004), Zupke et al. (1995), López-Soriano et al. (2004), Wright et al. (1992)
$\overline{Cit}$	0.400	mM	Armson and Mendis (1995), Bergmeyer (1974), Garfinkel (1971a), Howarth et al. (2004), Sies (1982), Wright et al. (1992), Zupke et al. (1995)
$\overline{AcCoA}$	0.070	mM	Bergmeyer (1974), Garfinkel (1971a), Greenhaff et al. (2002), Sies (1982), Putman et al. (1999), Wright et al. (1992), Ricny and Tucek (1980), Yeh et al. (1981)
$\overline{KG}$	0.250	mM	Bergmeyer (1974), Foulkes (1955), Garfinkel (1971a), Laplante et al. (1995), Ricny and Tucek (1980), Sies (1982), Wright et al. (1992)
$\overline{OAA}$	0.005	mM	Armson and Mendis (1995), Bergmeyer (1974), Garfinkel (1971a), Laplante et al. (1995), Sies (1982), Wright et al. (1992), Zupke et al. (1995)
$\overline{NAD}$	0.940	mM	Bergmeyer (1974), Garfinkel (1971a)
$\overline{ATP}$	3.230	mM	Armson and Mendis (1995), Bergmeyer (1974), Ricny and Tucek (1980)
$\overline{\Delta\psi}$	150	mV	Guérin (2004), Holian and Wilson (1980)
$\overline{v_{resp}}$	0.076	mM s⁻¹	Anflous et al. (1977), Saks et al. (2001)
$\overline{v_{ATP}}$	0.174	mM s⁻¹	Anflous et al. (1977)

[a] The concentrations listed in Table 1 are all given in mM, whereas in the referenced articles they are often given in μmol/(g fresh weight), μmol/(g dry weight) or μmol/(g protein). In order to have all those concentrations in mM, we collected values that gave us an idea of the converting factors: we used literature values for the ratio dry weight/fresh weight (Zeidan et al., 2000; Andersen et al., 2005; Hesselink et al., 2005; Pennisi et al., 2004; Arai et al., 2001; Viant et al., 2003; Bagshaw and Farquharson, 2002; Sies, 1982; Wright et al., 1992), cell volumes (Ohanna et al., 2005; Schneider et al., 1997; Rosenblad et al., 1999; Chin et al., 2000; Stamenovic et al., 2002; Rouzaire-Dubois and Dubois, 1998; Attene-Ramos et al., 2005; Metzler, 1978) and values for the ratio cytoplasm volume/dry weight (Sies, 1982). Even though these values were determined for different organisms, the average should be a good approximation. Conversion factors: μmol/(g fresh weight) into mM: 1.19; μmol/(g dry weight) into mM: 0.35; μmol/(g protein) into mM: 0.25. For some of the concentrations, when necessary, we used a mitochondrial volume/cytoplasm volume ratio of 0.18 (Sies, 1982; Wright et al., 1992).

Table 2
Constants of the model.

Species	asp	glu	Pi	N_t	A_t	K_{app}	$K_{6,eq}$[a]	C
Values in vivo	1.600	5.300	2.440	1.070	4.160	4.4e − 6	0.12	6.75e − 6
Unit	mM	mM	mM	mM	mM	Dimensionless	Dimensionless	mM mV^{-1}
References	Bergmeyer (1974), Garfinkel (1971a), Sies (1982), Wright et al. (1992)	Bergmeyer (1974), Garfinkel (1971a), Howarth et al. (2004), Sies (1982), Wright et al. (1992), Zupke et al. (1995)	Armson and Mendis (1995), Sies (1982)	Bergmeyer (1974), Garfinkel (1971a)	Armson and Mendis (1995), Bergmeyer (1974), Sies (1982), Ricny and Tucek (1980)	Alberty (2000), Guynn and Veech (1973)	Alberty (1998), Cortassa et al. (2003), Sies (1982)	Gunter and Pfeiffer (1990), Wojtczak et al. (1986)

[a] The equilibrium constant of reaction (6) given here is defined as $K_{6,eq} = KG_{eq}Asp_{eq}/(OAA_{eq}Glu_{eq})$. From this value and the values for *asp* and *glu*, our equilibrium constant was calculated $K_{eq} = K_{6,eq}(Glu_{eq}/Asp_{eq})$.

The constants used in v_{resp} or v_{ATP}, $K = 2$ mM, $\Delta\psi_m = 150$ mV, $a = 0.100$ mV^{-1} and $b = 0.004$ mM^{-1} were chosen to fit the experimental results. Then, the other parameters were calculated in order to fit the steady state concentrations or rates. $k_1 - k_8$, k_{resp}, k_{ATP}, k_{leak} and k_{ANT} are rate constants. As we did not have experimental values for v_{leak} and v_{ANT}, we decided to fix k_1 and k_3 in order to obtain the same order of magnitude for all the rates at steady state. In order to obtain for the steady state the values given in Table 1, we calculated the other parameters as follows (where $\bar{x}$ denoted the x concentration at steady state):

$$k_2 = \frac{\overline{OAA}\ \overline{AcCoA}}{\overline{Pyr}\ \overline{NAD}}k_3, \quad k_4 = \frac{\overline{OAA}\ \overline{AcCoA}}{\overline{Cit}\ \overline{NAD}}k_3, \quad k_5 = \frac{\overline{v_{resp}} - 2\overline{OAA}\ \overline{AcCoA}k_3}{2\overline{KG}\ \overline{NAD}(A_t - \overline{ATP})},$$

$$k_6 = \frac{\overline{v_{resp}} - 4\overline{OAA}\ \overline{AcCoA}k_3}{2\left(\overline{OAA} - \frac{\overline{KG}}{K_{eq}}\right)}, \quad k_7 = \frac{k_1 - \overline{OAA}\ \overline{AcCoA}k_3}{\overline{Pyr}\ \overline{ATP}},$$

$$k_8 = \frac{k_1 - \overline{OAA}\ \overline{AcCoA}k_3}{\overline{OAA}}, \quad k_{ATP} = \frac{\overline{v_{ATP}}}{\left(\frac{2}{1+\exp(b(\overline{ATP} - ATP_{crit}(\overline{\Delta\psi})))} - 1\right)},$$

$$k_{resp} = \frac{\overline{v_{resp}}}{\frac{N_t - \overline{NAD}}{K + N_t - \overline{NAD}}\frac{1}{1+\exp(a(\overline{\Delta\psi} - \Delta\psi_m))}}, \quad k_{ANT} = \frac{2\overline{v_{ATP}} + \overline{v_{resp}} - 2k_1}{2\overline{ATP}},$$

$$k_{leak} = \frac{10\overline{v_{resp}} - 3\overline{v_{ATP}} - \overline{v_{ANT}}}{\overline{\Delta\psi}}. \tag{26}$$

As the values of the concentrations at steady state vary from 1 to 1000, the parameters of the model are not of the same order of magnitude. For this reason, the variables and the time are scaled according to

$$p = \frac{Pyr}{\overline{Pyr}}, \quad a = \frac{AcCoA}{\overline{AcCoA}}, \quad c = \frac{Cit}{\overline{Cit}}, \quad k = \frac{KG}{\overline{KG}},$$

$$o = \frac{OAA}{\overline{OAA}}, \quad n = \frac{NAD}{N_t}, \quad e = \frac{ATP}{A_t}, \quad s = \frac{\Delta\psi}{\Delta\psi_m},$$

$$\tau = \frac{k_1}{\overline{Pyr}}t, \tag{27}$$

which leads to a new system (31)–(38) (see Appendix).

3. Theoretical results and numerical simulations

Lemma 3.1. *For each set of non-negative initial conditions, system (16)–(23) admits a globally defined solution on $[0,\infty)$. Each of the solution components (except $\Delta\psi$) remains non-negative for all $t > 0$. It also verifies the constraints $NAD < N_t$ and $ATP < A_t$.*

Lemma 3.2. *System (16)–(23) admits at least one non-trivial steady state*

$$\overline{S} = (\overline{Pyr}, \overline{AcCoA}, \overline{Cit}, \overline{KG}, \overline{OAA}, \overline{NAD}, \overline{ATP}, \overline{\Delta\psi}).$$
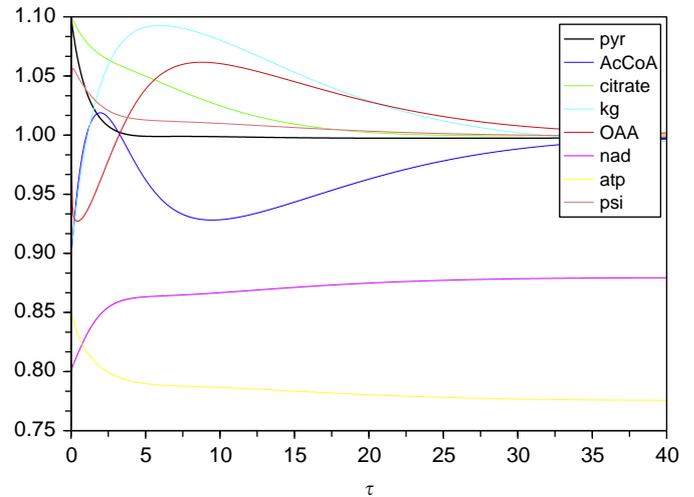

Fig. 6. Metabolite concentrations time course towards the steady state (initial conditions are taken as ±10% away from the steady state) with the following parameters: $\beta_2 \approx 0.60$, $\beta_3 \approx 0.53$, $\beta_4 \approx 0.60$, $\beta_5 \approx 2.41$, $\beta_6 \approx 0.42e - 3$, $\beta_7 \approx 0.61$, $\beta_8 \approx 0.47$, $\beta_{ANT} \approx 5.90$, $\beta_{leak} \approx 1.68$, $\beta_{resp} \approx 65.54$, $\beta_{ATP} \approx 3470.90$, $\delta_6 \approx 125.78$, $\delta_{r1} \approx 1.87$, $\delta_{r2} \approx 15$, $\delta_{atp} \approx 0.016$, $\delta_{crit} \approx 21.02$, $K'_{app} = 1.05e - 8$.

Proof of Lemmas 3.1 and 3.2. This follows from the transformation of system (16)–(23) to system (31)–(38) combined with Lemmas A.1 and A.2 (see Appendix).

Numerically, for any set of parameters and initial conditions, the system seems to have a unique global asymptotic steady state. This is shown in Figs. 6–8. In Fig. 6, the initial conditions are chosen at 10% away from the steady state. The steady state is rapidly reached after some damped oscillations. Fig. 7 depicts the case of low *ATP* concentration. This is a typical experimental situation when *ADP* is added to a suspension of mitochondria. *ATP* is synthesized at the expense of $\Delta\psi$ which drops rapidly, then recovers in the same time, as *ATP* is regenerated. This is exactly what is experimentally observed in these types of experiments. Usually the variations in concentration of TCA cycle metabolites are not recorded, so the single oscillation generated in this simulation has not yet been observed to our knowledge. However, it can easily be understood as the consequence of the fast decrease in *ATP* concentration. Then it propagates through $\Delta\psi$, *NADH* and the RC, and finally through *NADH* to the TCA cycle. It should be noticed, however, that most of the variations in TCA metabolites are (very) weak. In Fig. 8, the *ATP* concentration is higher than its steady state value so *ATP* hydrolyzes in *ADP* extruding protons and increasing $\Delta\psi$. Then $\Delta\psi$ returns slowly to its steady state value. Due to the increase in $\Delta\psi$ the rate of respiration is decreased, as deduced from the decrease in *NAD* concentration. All these
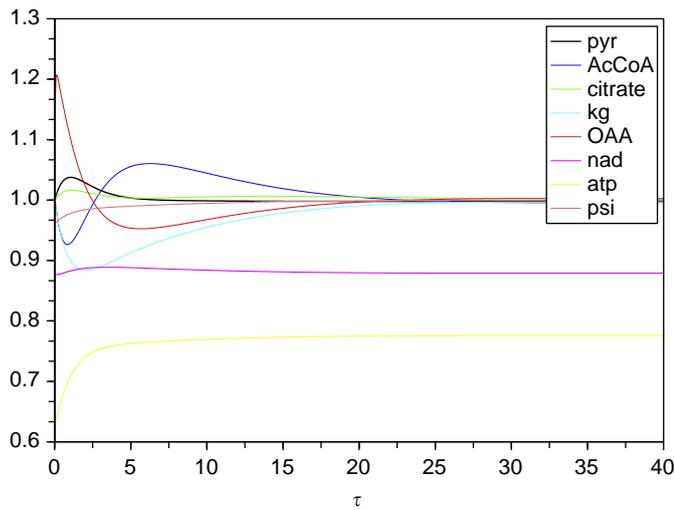
Fig. 7. Low ATP initial concentration (other initial values are taken as their steady state values).
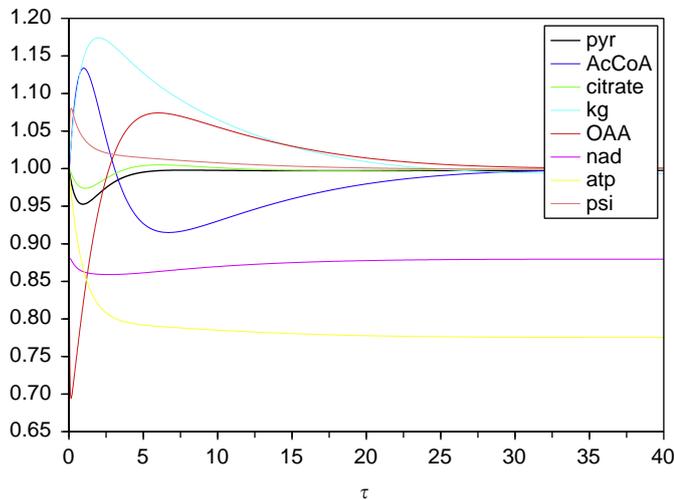

Fig. 8. High ATP initial concentration (other initial values are taken as their steady state values).

changes are accompanied by small damped oscillations of TCA cycle metabolites.

The parameters determined previously in Section 2.4 for an intermediate state of respiration have been used to simulate low and high ATP synthesis. For this aim k_{ANT} was varied keeping all other parameters constant. k_{ANT} deals with ATP/ADP carrier but can also represent the intensity of cell ATP consumption ($v_{ANT} = k_{ANT}ATP$). The results are represented in Table 3. When k_{ANT} is decreased (towards state 4) we observe an increase in ATP concentration, a decrease in NAD concentration, in respiration (v_{resp}) and in v_{ATP}. The reverse occurs when k_{ANT} is increased. The range of responses from 183 to 138 mV for $\Delta\psi$, from 3.98 to 2.22 mM for ATP, from 23.6 to 92.5 μM s^{-1} for v_{resp} and from 46.1 to 214.5 μM s^{-1} for v_{ATP} are in good agreement with the values of Table II in Bohnensack (1981).

In order to evaluate the effect of the reversibility of the other reactions, we have introduced a new term in the equations of v_3 and v_7 which are now:

$$v_3 = k_3\left(OAA\,AcCoA - \frac{Cit}{K_{3,eq}}\right), \quad v_7 = k_7\left(Pyr\,ATP - \frac{(A_t - ATP)OAA}{K_{7,eq}}\right),$$
(28)

Table 3
Steady state concentration values (in mM) and rates (in μM s^{-1}) at states 4, 3.5 and 3 with the following parameters: $k_1 = 38$ μM s^{-1}, $k_2 = 152$, $k_3 = 57\,142$, $k_4 = 53$, $k_7 = 40$ in (M s)$^{-1}$, $k_5 = 82\,361$ M^{-2} s^{-1}, $k_6 = 3.2e - 3$, $k_8 = 3.6$ in s^{-1}, $k_{resp} = 2.5$ $k_{atp} = 131.9$ mM s^{-1}, $k_l = 0.426$ M(mV s)$^{-1}$.

Species or rates	State 3	State 3.5	State 4
k_{ANT}	0.1	0.05387	0.005
$\overline{Pyr}$	0.161	0.140	0.185
$\overline{Cit}$	0.460	0.400	0.528
$\overline{AcCoA}$	0.105	0.070	0.019
$\overline{KG}$	0.146	0.250	0.693
$\overline{OAA}$	0.004	0.005	0.008
$\overline{NAD}$	0.968	0.940	0.309
$\overline{ATP}$	2.227	3.230	3.982
$\overline{\Delta\psi}$	138	150	183
$\overline{v_2} = \overline{v_3} = \overline{v_4}$	23.7	20	8.7
$\overline{v_5}$	22.5	18	3.1
$\overline{v_6}$	−1.2	−2	−5.6
$\overline{v_7} = \overline{v_8}$	14.3	18	29.3
$\overline{v_l}$	58.9	64	78.2
$\overline{v_{ANT}}$	222.7	174	19.9
$\overline{v_{resp}}$	92.5	76	23.6
$\overline{v_{ATP}}$	214.5	174	46.1

where $K_{3,eq} = 1e6/CoASH_{eq}$ (Lehninger Biochemistry, 1977), $K_{7,eq} = 1/Pi_{eq}$ (Lehninger Biochemistry, 1977), with $CoASH_{eq} \approx 10^{-3}$ mM (Sies, 1982). With these new reversible equations we show that we are still able to obtain the steady state corresponding to the physiological concentrations of TCA-cycle metabolites and to the intermediate rate of respiration, ATP synthesis and transmembrane potential summarized in Table 1. With this model it is still possible to reach states 4 and 3 and the results are the same as in Table 3.

4. Discussion

This simple model accounts at least qualitatively for the salient features of the oxidative phosphorylation system, namely:

- The coupling between the ATP synthesis and the RC and the coupling between the RC and the TCA cycle. When there is a demand in ATP (low ATP in Fig. 7), ATP is synthesized at the expense of $\Delta\psi$. The decrease in $\Delta\psi$ leads to an increase in the rate of respiration, which increases the demand in NADH supply by the TCA cycle.
- On the contrary, an excess of ATP is hydrolyzed, increasing the $\Delta\psi$ and decreasing the rate of respiration and the TCA cycle turn-over. This situation is encountered experimentally in cells lacking mitochondrial DNA (ρ^0 cells) (Dupont et al., 1985).
- The steady state appears numerically unique and stable, as is the case in the in vivo system. However, the variations seem more rapid than in the in vivo system. This could be due to the absence of other ions than protons giving rise to coupled exchange of ions slowing down all the processes. It could also be due to the absence of buffers of these ions (including protons) in our model. It is well known that the polar parts of phospholipids and proteins can bind ions. Special proteins can even complex some specific ions like calcium. The buffering power of ions might smooth and slow down the variations, particularly the damped oscillations.

However, several simplifying assumptions at the basis of the model can be questioned.

- The use of mass action kinetics is a very strong simplification. It has the great advantage of making an analytical processing possible, but one can argue that saturation is a key feature of biological reactions. We have nevertheless introduced a hyperbolic kinetic for NADH dehydrogenase (in v_{resp}) because it is the main output flux. This is clear from Table 3 in which v_{resp} is varied from a low value to a value close to its maximum. At the same time the rates in TCA cycle vary reasonably, between 8.7 and 23.9 for $v_2 = v_3 = v_4$ and between 3.1 and 22.5 for v_5.

- Irreversible reactions and regulations.

  The main reason for not introducing reversible reactions or regulation was the same as above, i.e. to work with a mathematically tractable model. As our aim was to obtain a simple model describing the links between the variations of TCA cycle when the oxidative phosphorylations are varied according to different cell ATP demands, we took as simple equations as possible. It means that we did not introduce regulations and took irreversible reactions even for some reversible reactions, but which always have the same direction in physiological conditions. This is the case for example of pyruvate carboxylase which is reversible but "formation of pyruvate from oxaloacetate by reversal of this process is unlikely since the intracellular concentration of oxaloacetate is very small" (Lehninger Biochemistry, 1977). We take great care in our fitting procedure to start with very low oxaloacetate concentrations (see Table 1) and we checked that this concentration remains low in our simulation (Table 3). Reaction (5), which is taken as irreversible, is in fact partially reversible because oxaloacetate can be converted into α-ketoglutarate by reaction (6). In order to evaluate the effect of the reversibility of the other reactions, we have introduced a new term in the equation of v_3 and v_7. With these new reversible equations it is still possible to obtain the steady state corresponding to the physiological concentrations of TCA-cycle metabolites and to an intermediate rate of respiration, ATP synthesis and transmembrane potential listed in Table 1. With this model it is possible to reach states 4 and 3 (same results as in Table 3). A reversible model has the advantage of exhibiting some kind of regulation due to the reversible inhibitory effect of the products (Atkinson, 1990). In addition, a reversible model can be particularly useful to describe the effect of mutations that occur in mitochondrial diseases with accumulation of intermediate metabolites.

5. Conclusion

A simple model is useful for several reasons. First, because in many instances it is not necessary to cope with all the complexity of a biological system. For instance, in many models dealing with the mitochondrial synthesis of ATP, it is enough to know that this synthesis is coupled through the transmembrane potential $\Delta\psi$ to an increase in the rate of oxygen consumption and an acceleration of the TCA cycle. The coupling is more important to model than all the details of the ATP synthesis or the oxygen consumption themselves.

Secondly, the salient features of a system and their interrelationships are more apparent on a simple system. Here the salient features are the shape of v_{resp} as a function of $\Delta\psi$, which is the result of several complex mechanisms. In our model the interrelationships (coupling) between the three large sets of reactions, ATP synthesis, rate of oxygen consumption and TCA

cycle are more evident because each block is summarized in one or few reactions.

Another advantage of a very simple model is that it is more easily tractable from the mathematical point of view. However, for mathematical studies we still have to deal with a quite large system and for this reason we transformed it into a planar system. By this way, we managed to prove the existence of at least one steady state. Biologically and numerically it seems that the steady state is unique and is a global attractor for the system. However, some basic techniques of qualitative stability analysis, which are sometimes useful for large systems, fail with our model (see remark at the end of Appendix). Moreover, we chose a dimensionless system among the several possible ones and there are very different time scales (a very fast transient for $\Delta\psi$). Before applying a singular perturbation method, the system needs to be improved because the variations in $\Delta\psi$ are too rapid. In this paper, we have presented a very simple model which remains difficult to analyze mathematically. However, from the experimental point of view, we are tempted to add several features (reversibility of some reactions, regulations, etc.) to this model to take better the observed behaviors into account. The question then arises: until which point a simple model can be complexified? Where can the cursor be put? The answer will depend on the biological question to which the model is intended to respond, but it must be kept in mind that very simple models are nevertheless able to exhibit many salient features of the biological reality.

Appendix A

A.1. Dimensionless system

With the new scaled variables, the rate equations become

$$v_1 = 1, \quad v_2 = \beta_2 p\,n, \quad v_3 = \beta_3 o\,a, \quad v_4 = \beta_4 c\,n, \quad v_5 = \beta_5 k\,n(1-e),$$
$$v_6 = \beta_6(o - \delta_6 k), \quad v_7 = \beta_7 p\,e, \quad v_8 = \beta_8 o, \quad v_{ANT} = \beta_{ANT} e,$$
$$v_{leak} = \beta_{leak} s,$$
$$v_{resp} = \beta_{resp} \frac{1-n}{(\delta_{r1} + 1 - n)} \frac{1}{1 + \exp(\delta_{r2}(s-1))},$$
$$v_{ATP} = \beta_{ATP}\left(\frac{2}{1 + \exp(\delta_{atp}(e - e_{crit}(s)))} - 1\right),$$
$$e_{crit} = \frac{K'_{app}}{K'_{app} + \exp(-\delta_{crit} s)}, \tag{29}$$

where the normalized constants are

$$\beta_2 = \frac{k_2}{k_1} N_t \overline{Pyr}, \quad \beta_3 = \frac{k_3}{k_1} \overline{OAA}\, \overline{AcCoA}, \quad \beta_4 = \frac{k_4}{k_1} N_t \overline{Cit}, \quad \beta_5 = \frac{k_5}{k_1} N_t A_t \overline{KG},$$
$$\beta_6 = \frac{k_6}{k_1} \overline{OAA}, \quad \beta_7 = \frac{k_7}{k_1} A_t \overline{Pyr},$$
$$\beta_8 = \frac{k_8}{k_1} \overline{OAA}, \quad \beta_{ANT} = \frac{k_{ANT}}{k_1} A_t, \quad \beta_{leak} = \frac{k_{leak}}{k_1} \Delta\psi_m, \quad \beta_{resp} = \frac{k_{resp}}{k_1},$$
$$\beta_{ATP} = \frac{k_{ATP}}{k_1},$$
$$\delta_6 = \frac{\overline{KG}}{\overline{OAA}\,K_{eq}}, \quad \delta_{r1} = \frac{K}{N_t}, \quad \delta_{r2} = a\Delta\psi_m, \quad \delta_{atp} = b\,A_t,$$
$$\delta_{crit} = 3\frac{1.2 F \Delta\psi_m}{RT}, \quad K'_{app} = K_{app} Pi. \tag{30}$$

The set of differential equations expressing the variation of the scaled variables is

$$\frac{dp}{d\tau} = v_1 - v_2 - v_7, \tag{31}$$

$$\varepsilon_1 \frac{da}{d\tau} = v_2 - v_3, \tag{32}$$

$$\varepsilon_2 \frac{dc}{d\tau} = v_3 - v_4, \tag{33}$$

$$\varepsilon_3 \frac{dk}{d\tau} = v_4 + v_6 - v_5, \tag{34}$$

$$\varepsilon_4 \frac{do}{d\tau} = v_5 + v_7 - v_3 - v_8 - v_6, \tag{35}$$

$$\varepsilon_5 \frac{dn}{d\tau} = -v_2 - v_4 - 2v_5 + v_{resp}, \tag{36}$$

$$\varepsilon_6 \frac{de}{d\tau} = v_{ATP} - v_{ANT} + v_5 - v_7, \tag{37}$$

$$\varepsilon_7 \frac{ds}{d\tau} = 10v_{resp} - 3v_{ATP} - v_{leak} - v_{ANT} \tag{38}$$

with

$$\varepsilon_1 = \frac{\overline{AcCoA}}{Pyr}, \quad \varepsilon_2 = \frac{\overline{Cit}}{Pyr}, \quad \varepsilon_3 = \frac{\overline{KG}}{Pyr}, \quad \varepsilon_4 = \frac{\overline{OAA}}{Pyr}, \quad \varepsilon_5 = \frac{N_t}{Pyr},$$

$$\varepsilon_6 = \frac{A_t}{Pyr}, \quad \varepsilon_7 = \frac{\Delta\psi_m}{Pyr} C. \tag{39}$$

A.2. Mathematical results

Lemma A.1. *For each set of non-negative initial conditions, system (31)–(38) admits a globally defined solution on $[0, \infty)$. Each of the solution components (except s) remains positive for all $t > 0$. It also verifies the constraints $n < 1$ and $e < 1$.*

Proof. Local existence and uniqueness on some maximal time interval is straightforward by using the Cauchy–Lipschitz theorem. Since the initial conditions are non-negative, and the vector field defined by the right hand side of (31)–(37) at the boundary of the region $\mathbb{R}^7_+$ never points outwards, all the concentrations $p, \ldots, n$ remain non-negative for all τ.

If $e = 1$ then according to the dimensionless rate equation (29), we have $e > e_{crit}$ and then $v_{ATP} < 0$. Since $\varepsilon_6(de/d\tau) = v_{ATP} - v_{ANT} - \beta_7 p < 0$, it follows that e decreases. Consequently, if $0 < e(0) < 1$ we have $0 < e < 1$.

By the same reasoning, we show that $n < 1$ because $v_{resp}(1, s) = 0$.

Set $S = p + \varepsilon_1 a + \varepsilon_2 c + \varepsilon_3 k + \varepsilon_4 o$, since $(dS/d\tau) = 1 - v_3 - v_8$, we have $S(\tau) < S(0) + \tau$.

For s, we have $\varepsilon_7(ds/d\tau) = f(\tau) - \beta_{leak} s$ where $f(\tau) = 10v_{resp} - 3v_{ATP} - v_{ANT}$ is bounded.

So $\varepsilon_7 s(\tau) = s(0)e^{-\beta_{leak}\tau} + \int_0^\tau f(u)e^{-\beta_{leak}(\tau-u)} du$ and we obtain $|\varepsilon_7 s(\tau)| \leqslant s(0)e^{-\beta_{leak}\tau} + M$.

So S and s cannot be infinite in finite time. Therefore, solutions to the system exist globally in time.

Lemma A.2. *There is at least one non-trivial steady state $\overline{S} = (\overline{p}, \overline{a}, \overline{c}, \overline{k}, \overline{o}, \overline{n}, \overline{e}, \overline{s})$ for system (31)–(38).*

Proof. From (31), we derive at steady state

$$\overline{p} = \frac{1}{\beta_2 n + \beta_7 e}.$$

Adding the right hand side of (32) and (33), we obtain

$$\overline{c} = \frac{\beta_2}{\beta_4(\beta_2 n + \beta_7 e)}.$$

Similarly, with (33)–(35), we have

$$\overline{o} = \frac{\beta_7 e}{\beta_8(\beta_2 n + \beta_7 e)}.$$

With (31)–(35), we find

$$\overline{a} = \frac{\beta_2 \beta_8 n}{\beta_3 \beta_7 e}$$

from (34),

$$\overline{k} = \frac{(\beta_2 \beta_8 n + \beta_6 \beta_7 e)}{\beta_8(\beta_2 n + \beta_7 e)(\beta_6 \delta_6 + \beta_5 n(1 - e))}$$

and adding $(36) - \frac{1}{10}(38) - \frac{3}{10}(37)$, we obtain

$$\overline{s} = \frac{10}{\beta_{leak}}\left(2\beta_2 \overline{p}n + \frac{23}{10}\beta_5 \overline{k}n(1 - e) - \frac{4\beta_{ANT}}{10}e - \frac{3}{10}\beta_7 \overline{p}e\right).$$

Therefore, the existence of a steady state is related to the existence of (n, e) satisfying $(f_1, f_2)(n, e) = (0, 0)$ with

$$f_1(n, e) = -\beta_2 \overline{p}n - \beta_4 \overline{c}n - 2\beta_5 \overline{k}n(1 - e) + v_{resp}$$

and

$$f_2(n, e) = v_{ATP} - v_{ANT} + \beta_5 \overline{k}n(1 - e) - \beta_7 \overline{p}e.$$

Now we prove that such (n, e) exists. Let us define the function $F = (f_1, f_2)$. Since $f_1(0, e) = v_{resp} > 0$, $f_1(1, e) < 0$, $f_2(n, 0) = v_{ATP}(n, 0) > 0$ and $f_2(n, 1) = v_{ATP}(n, 1) - k_{ANT} - \beta_7 p < 0$, then F vanishes at least once on $]0, 1[\times]0, 1[$. In order to verify this, we apply Lemma A.3. $\square$

Lemma A.3. *If $F = (f_1, f_2) : \mathbb{R}^2 \leftarrow \mathbb{R}^2$ is a continuous vector field such that*

$$f_1(0, e) > 0 \quad f_1(1, e) < 0 \quad \forall e \in [0, 1], \tag{40}$$
$$f_2(n, 0) > 0 \quad f_2(n, 1) < 0 \quad \forall n \in [0, 1] \tag{41}$$

then there exists $\overline{m} = (\overline{n}, \overline{e})$ which satisfies

$$0 < \overline{n} < 1, \quad 0 < \overline{e} < 1, \quad F(\overline{m}) = 0.$$

Proof. Let us note the square $C = \{(n, e) \in \mathbb{R}^2; 0 < n < 1, 0 < e < 1\}$ and define the following homotopy

$$H^\tau(n, e) = (1 - \tau)F(n, e) + \tau G(n, e), \quad \tau \in [0, 1] \tag{42}$$

with $G(n, e) = (\frac{1}{2} - n, \frac{1}{2} - e)$. From the assumption on F, for all $\tau \in [0, 1]$, F never vanishes on ∂C. We can define the degree of H^τ and using homotopy invariance we have

$$deg(H^\tau, C, 0) = deg(H^0, C, 0) = deg(H^1, C, 0). \tag{43}$$

As $H^1 = G$ and G vanishes only on $(\frac{1}{2}, \frac{1}{2})$, we obtain

$$deg(H^1, C, 0) = sign\left(\det\left(J_G\left(\frac{1}{2}, \frac{1}{2}\right)\right)\right) = 1 \neq 0, \tag{44}$$

where $sign(\det(J_G(\frac{1}{2}, \frac{1}{2})))$ is the sign of the determinant of the jacobian of G at $(\frac{1}{2}, \frac{1}{2})$. Since the degree of $H^0 = F$ is not equal to zero, F vanishes at leat once inside C (Smoller, 1994, Section A, Chapter 12). $\square$

Remark. If F is not continuous at $(0,0)$, the same result holds by applying the same argument to the function on the smaller square $[\varepsilon, 1] \times [\varepsilon, 1]$.

Remark. Let us denote $J = (a_{ij})_{1 \leqslant i,j \leqslant 8}$ the Jacobian at steady state. The system is not qualitatively stable (because $a_{ij}a_{ji}$ can be positive for some (i, j), i.e. the members of some given interacting species do not have opposite effects on each other). However, it seems that the magnitudes of interaction are appropriately balanced. Unfortunately, J is not also diagonally dominant (i.e. there are not n numbers $d_n > 0$ such that $a_{ii}d_i + \sum_{j \neq i}|a_{ij}|d_j < 0$ $\forall i = 1, \ldots, n$).

References

Alberty, R., 2000. Calculating apparent équilibrium constants of enzyme-catalyzed reactions at pH 7. Biochem. Educ. 28, 12–17.

Alberty, R.A., 1998. Calculation of standard transformed formation properties of biochemical reactants and standard apparent reduction potentials of half reactions. Arch. Bioch. Biophys. 358 (1), 25–39.

Andersen, J.B., Rourke, B.C., Caiozzo, V.J., Bennett, A.F., Hicks, J.W., 2005. Physiology: postprandial cardiac hypertrophy in pythons. Nature 434, 37–38.

Anflous, K., Veksler, V., Mateo, P., Samson, F., Saks, V., Ventura-Clapier, R., 1997. Mitochondrial creatine kinase isoform expression does not correlate with its mode of action. Biochem. J. 322, 73–78.

Arai, K., Lee, K., Berthiaume, F., Tompkins, R.G., 2001. Intrahepatic amino acid and glucose metabolism in a D-galactosamine-induced rat liver failure model. Hepatology 34 (2), 360–361.

Armson, A., Mendis, A.H., 1995. Steady state content of glycolytic/tricarboxylic acid-cycle intermediates, adenine nucleotide pools and the cellular redox-status in the infective (L3) larvae of (homogonic) Strongyloides ratti. Int. J. Parasitol. 25 (2), 197–202.

Atkinson, D.E., 1990. What should a theory of metabolic control offer to the experimenter? In: Cornish-Bowden, A., Cardenas, M.L. (Eds.), Control of Metabolic Processes. Springer, Berlin, pp. 3–11.

Attene-Ramos, M.S., Kitiphongspattana, K., Ishii-Schrade, K., Gaskins, H.R., 2005. Temporal changes of multiple redox couples from proliferation to growth arrest in IEC-6 intestinal epithelial cells. Am. J. Physiol. Cell Physiol. 289 (5), C1220–C1228.

Bagshaw, A.P., Farquharson, M.J., 2002. Simultaneous determination of iron, copper and zinc concentrations in skin phantoms using XRF spectrometry. X-Ray Spectrom. 31 (1), 47–52.

Beard, D.A., 2005. A biophysical model of the mitochondrial respiratory system and oxidative phosphorylation. Plos Comput. Biol. 1, 252–264.

Berg, J.M., Tymoczko, J., Stryer, L., 2006. Biochemistry. Freeman, New York.

Bergmeyer, H.U., 1974. Methods of Enzymatic Analysis. Verlag Chem. Int., Weinheim.

Bohnensack, R., 1981. Control of energy transformation of mitochondria. Analysis by a quantitative model. Biochim. Biophys. Acta 634, 203–218.

Chin, J., Miller, S.C., Wada, M., Nagano, N., Nemeth, E.F., Fox, J., 2000. Activation of the calcium receptor by a calcimimetic compound halts the progression of secondary hyperparathyroidism in uremic rats. J. Am. Soc. Nephrol. 11, 903–911.

Cortassa, S., Aon, M.A., Marbán, E., Winslow, R.L., O'Rourke, B., 2003. An integrated model of cardiac mitochondrial energy metabolism and calcium dynamics. Biophys. J. 84 (4), 2734–2755.

Dupont, C.H., Mazat, J.P., Guerin, B., 1985. The role of adenine nucleotide translocation in the energization of the inner membrane of mitochondria isolated from rho + and rho degree strains of Saccharomyces cerevisiae. Biochem. Biophys. Res. Commun. 132 (3), 1116–1123.

Foulkes, E.C., 1955. Studies in cell permeability, the uptake of pyruvate by yeast. J. Gen. Physiol. 38 (4), 425–430.

Garfinkel, D., 1971a. Simulation of the Krebs cycle and closely related metabolism in perfused rat liver. I. Construction of a model. Comput. Biomed. Res. 4 (1), 1–17.

Garfinkel, D., 1971b. Simulation of the Krebs cycle and closely related metabolism in perfused rat liver. II. Properties of the model. Comput. Biomed. Res. 4 (1), 18–42.

Greenhaff, P.L., Campbell-O'Sullivan, S.P., Constantin-Teodosiu, D., Poucher, S.M., Roberts, P.A., Timmons, J.A., 2002. An acetyl group deficit limits mitochondrial ATP production at the onset of exercise. Biochem. Soc. Trans. 30 (2), 275–280.

Guérin, B., 2004. Bioénérgetique. EDP Sciences, Grenoble, p. 166.

Gunter, T.E., Pfeiffer, D.R., 1990. Mechanisms by mitochondria transport calcium. Am. J. Physiol. 258, C755–C786.

Guynn, R.W., Veech, R.L., 1973. The equilibrium constants of the adenosine triphosphate hydrolysis and the adenosine triphosphate–citrate lyase reactions. J. Biol. Chem. 248 (20), 6966–6972.

Hesselink, R.P., Van Kranenburg, G., Wagenmakers, A.J., Van der Vusse, G.J., Drost, M.R., 2005. Age related decline in muscle strength and power output in 1-4-a-glucosidase knockout mice. Muscle Nerve 31 (3), 374–381.

Holian, A., Wilson, D.F., 1980. Relationship of transmembrane pH and electrical gradients with respiration and adenosine 5′-triphosphate synthesis in mitochondria. Biochemistry 19 (18), 4213–4221.

Howarth, K.R., LeBlanc, P.J., Heigenhauser, G.J., Gibala, M.J., 2004. Effect of endurance training on muscle TCA cycle metabolism during exercise in humans. J. Appl. Physiol. 97 (2), 579–584.

Kondracheva, M.N., Doliba, N.M., 1989. Polarographic observation of substrate-level phosphorylation and its stimulation by acetylcholine. FEBS Lett. 243, 153–155.

Korzeniewski, B., 1991. An extended dynamic model of oxidative phosphorylation. Biochim. Biophys. Acta 1060 (2), 210–223.

Korzeniewski, B., Malgat, M., Letellier, T., Mazat, J.P., 2001. Effect of 'binary mitochondrial heteroplasmy' on respiration and ATP synthesis: implications for mitochondrial diseases. Biochem. J. 357, 835–842.

Laplante, A., Compte, B., Des Rosiers, C., 1995. Assay of blood and tissue oxaloacetate and α-ketogluterate by isotope dilution gas chromatography–mass spectrometry. Anal. Biochem. 224 (2), 580–587.

Lehninger Biochemistry, second edition. Worth Publisher, New York, 1977.

López-Soriano, J., Carbó, N., Almendro, V., Figueras, M., Ribas, V., Busquets, S., López-Soriano, F.J., 2004. Rat liver lipogenesis is modulated by interleukin-15. Int. J. Mol. Med. 13 (6), 817–819.

Magnus, G., Keizer, J., 1997. Minimal model of β-cell mitochondrial Ca^{2+}-handling. Am. J. Physiol. Cell. Physiol. 273, C717–C733.

Metzler, D.E., 1978. Biochemistry: The Chemical Reactions of Living Cells, second ed. Harcourt Academic Press, New York.

Ohanna, M., Sobering, A.K., Lapointe, T., Lorenzo, L., Praud, C., Petroulakis, E., Sonenberg, N., Kelly, P.A., Sotiropoulos, A., Pende, M., 2005. Atrophy of S6K1 (-/-) skeletal muscle cells reveals distinct mTOR effectors for cell cycle and size control. Nat. Cell Biol. 7 (3), 286–294.

Parlo, R.A., Coleman, P.S., 1984. Enhanced rate of citrate export from cholesterol-rich hepatoma mitochondria. J. Biol. Chem. 259, 9997–10003.

Pennisi, P.A., Kopchick, J.J., Thorgeirsson, S., LeRoith, D., Yakar, S., 2004. Role of growth hormone(GH)in liver regeneration. Endocrinology 145 (10), 4748–4755.

Putman, C.T., Matsos, M.P., Hultman, E., Jones, N.L., Heigenhauser, G.J., 1999. Pyruvate dehydrogenase activation in active muscle during and after maximal exercise in men. Am. J. Physiol. Endocrinol. Metab. 276 (3), E483–E488.

Ricny, J., Tucek, S., 1980. Relation between the content of acetyl-coenzyme A and acetylchloline in brane slices. Biochem. J. 188 (3), 683–688.

Rosenblad, C., Kirik, D., Björklund, A., 1999. Neurturin enhances the survival of intrastriatal fetal dopaminergic transplants. NeuroReport 10 (8), 1783–1887.

Rouzaire-Dubois, B., Dubois, J.M., 1998. K+ channel block-induced mammalian neuroblastoma cell swelling: a possible mechanism to influence profliferation. J. Physiol. 510, 93–102.

Rustin, P., Bourgeron, T., Parfait, B., Chretien, D., Munnich, A., Rotig, A., 1997. Inborn errors of the Krebs cycle: a group of unusual mitochondrial diseases in human. Biochim. Biophys. Acta 1361, 185–197.

Saks, V.A., Kaambre, T., Sikk, P., Eimre, M., Orlova, E., Paju, K., Piirsoo, A., Appaix, F., Kay, L., Regitz-Zagrosek, V., Fleck, E., Seppet, E., 2001. Intracellular energetic units in red muscle cells. Biochem. J. 356, 643–657.

Schneider, S.W., Yano, Y., Sumpio, B.E., Jena, B.P., Geibel, J.P., Gekle, M., Oberleithner, H., 1997. Rapid aldosterone-induced cell volume increase of endothelial cells measured by the atomic force microscope. Cell Biol. Int. 21 (11), 759–768.

Segel, I., 1975. Enzyme Kinetics: Behavior and Analysis of Rapid Equilibrium and Steady State Enzyme Systems. Wiley, New York.

Sies, H., 1982. Metabolic Compartimentation. Academic Press, London, 123–146 and 235–257.

Smoller, J., 1994. Shock Waves and Reaction-Diffusion Equations, second ed. Springer, Berlin.

Stamenovic, D., Mijailovich, S.M., Tolic-Norrelykke, I.M., Chen, J., Wang, N., 2002. Cell prestress. II. Contribution of microtubules. Am. J. Physiol. Cell Physiol. 282 (3), C617–C624.

Viant, M.R., Rosenblum, E.S., Tieerdema, R.S., 2003. NMR-based metabolomics: a powerful approach for characterizing the effects of environmental stressors on organism health. Environ. Sci. Technol. 37 (21), 4982–4989.

Wilson, D.F., Owen, C.S., Holian, A., 1977. Control of mitochondrial respiration: a quantitative evaluation of the roles of cytochrome c and oxygen. Arch. Biochem. Biophys. 182 (2), 749–762.

Wojtczak, L., Zolkiewska, A., Duszynski, J., 1986. Energy-storage capacity of the mitochondrial proton-motive force. Biochim. Biophys. Acta 851 (2), 313–321.

Wright, B.E., Butler, M.H., Albe, K.R., 1992. Systems analysis of the tricarboxylic acid cycle in Dictyostelium discoideum. I. The basis for model construction. J. Biol. Chem. 267 (5), 3101–3105.

Wu, F., Yang, F., Vinnakota, K.C., Beard, D.A., 2007. Computer modelling of mitochondrial tricarboxylic cycle, oxidative phosphorylation, metabolite transport, and electrophysiology. J. Biol. Chem. 282 (34), 24525–24537.

Yeh, L.A., Song, C.S., Kim, K.H., 1981. Coenzyme A activation of acetyl-CoA carboxylase. J. Biol. Chem. 256 (5), 2289–2296.

Zeidan, A., Nordström, I., Dreja, K., Malmqvist, U., Hellstrand, P., 2000. Stretch-dependent modulation of contractility and growth in smooth muscle of rat portal vein. Circ. Res. 87 (3), 228–234.

Zupke, C., Sinskey, A.J., Stephanopoulos, G., 1995. Intracellular flux analysis applied to the effect of dissolved oxygen on hybridomas. Appl. Microbiol. Biotechnol. 44 (1–2), 27–36.